Conf-930408--65

SAND92-2670C

INVESTIGATION OF FRACTURE-MATRIX INTERACTION: PRELIMINARY EXPERIMENTS IN A SIMPLE SYSTEM

S. D. Foltz
University of New Mexico
Department of Physics and Astronomy
Albuquerque, New Mexico 87131

V. C. Tidwell and R. J. Glass
Geoscience Center
Sandia National Laboratories
Albuquerque, New Mexico 87185

S. R. Sobolik
YMP Performance Assessment Applications
Sandia National Laboratories
Albuquerque, New Mexico 87185

SAND--92-2670C

DE93 011580

ABSTRACT

Paramount to the modeling of unsaturated flow and transport through fractured porous media is a clear understanding of the processes controlling fracture-matrix interaction. As a first step toward such an understanding, two preliminary experiments have been performed to investigate the influence of matrix imbibition on water percolation through unsaturated fractures in the plane normal to the fracture. Test systems consisted of thin slabs of either tuff or an analog material cut by a single vertical fracture into which a constant fluid flux was introduced. Transient moisture content and solute concentration fields were imaged by means of x-ray absorption. Flow fields associated with the two different media were significantly different owing to differences in material properties relative to the imposed flux. Richards' equation was found to be a valid means of modeling the imbibition of water into the tuff matrix from a saturated fracture for the current experiment.

INTRODUCTION

Estimates of groundwater travel time through the unsaturated zone at Yucca Mountain, a critical factor in evaluating the suitability of the potential high-level radioactive waste repository, are very sensitive to the nature and degree of fracture-matrix interaction. Fracture-matrix interaction refers to the transfer of fluids and solutes between fractures and the porous matrix of an unsaturated rock mass. Such interaction plays a significant role in the way flow and transport processes are modeled under

both transient and steady flow conditions. For example, current conceptual models make significant assumptions concerning the nature of fracture-matrix interaction. Composite continuum models do not explicitly address fracture-matrix interaction but lump the influence of such processes into effective properties.[1] Dual porosity models treat the fractured medium as two overlapping, interacting continua with the interaction between the fracture and matrix continua being modeled by a "leakage" or transfer function.[2,3] Fractures and matrix may also be modeled discretely, by explicitly addressing boundary conditions at the fracture-matrix interface.[4,5]

The development and evaluation of conceptual models for flow and transport in fractured unsaturated rock is best accomplished in conjunction with physical observation in the field and systematic experimentation within a controlled laboratory setting.[6,7] In reviewing experiments that have been conducted, one finds that they often uncover nuances of the physical system that modeling accomplished independent of experimental work cannot achieve. Russo and Reda[8] found that microfractures too small to be detected visually, have significant effects on the transient moisture distribution in a core of tuff. Glass and Norton[9] found significant air entrapment and hysteresis in a horizontal fracture saturated from the matrix. Nicholl, Glass and Nugyen[10,11,12] found gravity-driven infiltration flow instability in non-horizontal fractures to form downward growing fingers during infiltration events. Gallegos et al.[13] found naturally occurring fracture coatings to significantly effect matrix absorption. During laboratory fracture-matrix imbibition investigations, Rasmussen[14] noted visual differences in matrix saturation along the edge of a block of tuff containing a horizontal fracture which was believed to be caused by channelling of water within the unsaturated fracture.

Here we present the results of preliminary laboratory scale fracture-matrix imbibition experiments that investigate interaction normal to the plane of a vertical fracture. Thin slab fracture-matrix systems were constructed out of tuff and an analog material. Transient water saturation and solute concentration fields were recorded using a high resolution full-field

moisture content measurement technique based on x-ray absorption principles.[15] The influence of matrix heterogeneity on water imbibition in both the tuff and analog material is clearly evidenced. Moisture saturation fields were analyzed to test the validity of the Richards' equation for horizontal matrix imbibition from a saturated fracture. This analysis also determined the sorptivity of the matrix material for boundary conditions typical of near-surface conditions. The results of these experiments emphasizes the ability to apply a systematic investigative approach to research in fracture-matrix interaction.

EXPERIMENTAL METHOD

A single, vertical fracture was formed by placing two thin, oven-dried plates of porous media edge-to-edge. Narrow strips of stainless steel shim stock maintained an approximate 100 micron slotted gap between the plates during assembly. The two plates were first bridged with plastic laminant film applied with a hot iron. The laminated plates were then sandwiched between two sheets of parafilm, which provided mechanical rigidity upon cooling. A schematic of the test chamber is given in Figure 1.

Two types of porous plates were examined: volcanic tuff and an analog material consisting of sintered glass beads. The tuff plates (14.0 cm x 10.2 cm x 2.5 cm/plate) were cut from a block of Timber Mountain Tuff collected near Rainier Mesa on the Nevada Test Site. Petrographic inspection of the tuff identified it to be a partially welded and devitrified, high silica rhyolite with 10% phenocrysts of sanadine. Secondary calcite is found dispersed through the rock and likely affects the permeability. A porosity of 0.27 was measured gravimetrically on a small core of the tuff.

The analog porous media provides a chemically inert system manufactured to hydraulic specification, which can be cleaned and reused. Fabrication of the analog plates involves homogeneously packing[16] glass (soda-lime) beads into a graphite mold with inner dimensions of 15.2 cm x 10.2 cm x 0.8 cm. The plates are then fired in a nitrogen atmosphere furnace. The plates used in this experiment had a pre-sintering bead size distribution of 0.15 to 0.21

mm and were fired at 656°C for 696 min. The porosity of both plates was measured by gravimetric means to be approximately 0.30.

During the experiment, constant pressure boundary conditions were maintained around the edge of the slab to allow air to escape. The experiment was started by supplying a steady flow of potassium iodide (KI) solution (10% by weight) to the top of the vertical fracture. The solution was pumped at a constant rate of 1.7 ml/min through a 25 gauge needle inserted into a 1 mm I.D. capillary tube which was centered over the top of the fracture. KI was used to increase the x-ray absorption of the wetting solution and hence improve image contrast. A light suction imposed by aspiration was applied at the bottom of the fracture to prevent the build-up of fluid along the lower boundary. Thus the experiment simulated the top of a much longer fracture-matrix system.

Moisture content fields were captured incrementally in time during the transient water imbibition phase of the experiment using the x-ray adsorption method developed by Tidwell and Glass.[15] X-ray sensitive film (Kodak Industrial AA sheet film) was placed on the back of the fracture-matrix slab and exposed by an industrial x-ray unit set at 60 kilovolts and 18 miliamps (100 sec for tuff, 60 sec for analog to achieve optimum contrast).

Following complete saturation of the fracture-matrix system, the injection solution was switched to pure deionized water (DeI). A series of exposures were taken to explore the flushing of the KI solution from the fracture-matrix system. This component of the experiment was designed to demonstrate the capabilities of the x-ray absorption technique to image transient solute concentration fields.

Once the x-ray film was developed, a 512 x 512 array CCD camera and IBM 486 PC-based frame grabber were used to digitize the radiograph at 256 grey-levels of resolution. Using step-wedge information appearing in each image, data were adjusted for minor systematic variations in field strengths, film, and equipment characteristics.[15] X-ray absorption theory was used to convert each of the 262,144 data points within the two-dimensional field into saturation values.[15]

RESULTS AND DISCUSSION

Figures 2 and 3 show a sequence of saturation images for the analog and tuff fracture-matrix systems, respectively. In these images, white signifies 100% saturation grading to black corresponding to initial saturation (oven dry). It should be noted that the measurement technique has impacted the results shown here in two ways. First, saturation levels reported for the fracture are an artifact of the measurement technique. This effect is in part due to difficulties in imaging the fluid in the fracture while maintaining suitable contrast within the matrix. Difficulties in achieving precise registration of images, required when converting grey-level to saturation, is also to blame. However, image registration is a problem only when significant contrast differences exist across very fine structure such as a fracture. Influence of the experimental technique can also been seen in the increased widening of the wetted region as the lower boundary of the matrix is approached.

The imaging technique was evaluated by comparing the mass of solution introduced into the test system with that calculated from the saturation images. Only the mass of fluid pumped into the system was measured, hence comparisons must be drawn for images taken prior to breakthrough at the bottom of the fracture. In the tuff system breakthrough occurred almost immediately; therefore, comparison was only possible for the analog system. Figure 4 shows that reference and calculated volumes within the system agree closely.

Images of the solute concentration fields for the saturated analog system are shown in Figure 5. In these four images the grey scale qualitatively references solute concentration, with white signifying a concentration of 10% KI, while black corresponds to pure DeI. The shape of these fields as well as the sharp contrast in concentration suggest that displacement of the KI solution in the analog material was advectively driven. Dispersion evident in these images is primary an artifact of the integration of the position of the transient solute front over the 60 sec exposure time. A very different response was noted in the case of the tuff system where

very slow matrix diffusion was the dominant transport process. Images of the solute concentration fields showed no change from the initial state for the 60 minutes that the solute transport field was monitored and hence are not shown here.

Although similar boundary conditions and fracture characteristics were maintained, significant differences between the transient flow fields in the analog and tuff systems were observed. The most notable difference was the dominance of matrix flow in the analog system while fracture flow dominated in the tuff system. Matrix dominated flow in the analog material was induced by a number of factors. First, capillary forces in the matrix were sufficient to prevent the fracture from saturating until late in the experiment when the matrix approached full saturation. Once the fluid was imbibed by the matrix (near the top of the fracture), gravitational forces predominated directing the flow vertically in the matrix. Matrix flow was further aided by high permeability which was sufficient, under the imposed flux, to conduct the imbibed fluid entirely within the matrix. Although capillary forces of the tuff were stronger than for the analog, low matrix permeability of the tuff prevented substantial imbibition thus fracture flow predominated. Hydraulic properties of the sample were not measured, but given that permeabilities measured for similar tuff materials are generally low and that the analog material can be characterized as having a very open pore structure (due to the narrow grain size distribution, the size of the beads used, and short sintering time) significant differences in permeability are expected.

Heterogeneities had a pronounced effect on the flow field within both the tuff and analog systems. If the tuff system were homogeneous, the wetting front would have moved into the matrix essentially as a vertical front (parallel to the fracture) because the fluid in the fracture was maintained at near atmospheric pressure throughout the experiment. This clearly was not the case. Figure 3 shows the effect of two pumice nodules (upper part of image on either side of the fracture) containing large pores to slow flow and increase tortuosity under these unsaturated conditions. While this system response is expected, it points out the difference with saturated systems where such a

nodule would constitute a high conductivity material.

The analog system exhibits asymmetry about the fracture plane for both the imbibition and saturated solute transport tests. During the imbibition phase, higher imbibition into the right side plate occurred indicating slightly greater capillary forces and thus smaller pores in the right plate. With solute transport, the right dispersion front was retarded relative to the left, again indicating smaller pores in the right plate. Within each analog plate, however, both saturation and solute concentration fields indicate homogeneity.

MODEL VALIDATION EXERCISE

Saturation and solute concentration fields measured in our experiments can be used to test model validity. Here we perform a simple test with the water imbibition data from the tuff experiment to demonstrate the validity of Richard's equation for horizontal imbibition into a dry tuff matrix from a saturated fracture. This simple validation test can be carried out without approximate analytical theory, detailed property data, or complicated numerical code in the following way.

Richards' equation for horizontal flow may be written

$$\frac{\partial \theta}{\partial t} = \frac{\partial}{\partial z} D(\theta) \frac{\partial \theta}{\partial z} \qquad (1)$$

with boundary and initial conditions

x	t=0	$\theta=\theta_i$	
x=0	t>0	$\theta=\theta_o$	(2)
x	t>0	$\theta=\theta_i$	

Where $D(\theta)$ is the water diffusivity of the media. Equation (1) with (2) allow transformation to the non-linear ordinary differential equation

$$\frac{\xi}{2} \frac{d\theta}{d\xi} = \frac{d}{d\xi} D(\theta) \frac{d\theta}{d\xi} \qquad (3)$$

with the boundary conditions

$\xi=0$	$\theta=\theta_o$	
ξ	$\theta=\theta_i$	(4)

where ξ is the Boltzmann similarity variable given by $x/t^{\frac{1}{2}}$.

Even though (3) is non-linear, solutions to (3) with (4) for θ are dependent only on ξ regardless of the functional form of $D(\theta)$. To show that this equation provides an adequate model of system behavior, any given moisture value must propagate through the media with $t^{\frac{1}{2}}$ dependence. Such dependence is shown to be the case for the tuff experiment by means of the following two analyses.

Figure 6 shows a time series of saturation profiles taken normal to the fracture 9 cm below the top of the tuff fracture-matrix system. Values are averages of a moving window 11 pixels high and 5 pixels wide. A value of saturation of 0.5 was chosen and the distance (d) from the fracture was determined from each profile. A plot of d versus $t^{\frac{1}{2}}$ is found to be linear with small scatter as shown in figure 7. The slope of this line is simply $\xi(0.5)$ (i.e., the Boltzmann similarity variable for a saturation of 0.5).

Another check on the $t^{\frac{1}{2}}$ dependence is to calculate the total volume of water per unit cross-section of fracture in time as it too will show $t^{\frac{1}{2}}$ dependence. The total volume infiltrated per cross-sectional area of fracture (I), is determined for the same region by simply integrating over each of the profiles in the time series. Figure 8 shows a plot of I versus $t^{\frac{1}{2}}$ also to be linear. Half the slope of this line (because it is the combined effect of both sides of the fracture) is the sorptivity of the media which is the single media property required to model the total volume inflow and the imbibition rate from the fracture into the matrix. It must be noted that the sorptivity is defined as a function of boundary and initial conditions and applies within the context of equations (3) and (4).

This simple test serves as an example of validation for a subprocess of the fracture-matrix system; however, it has been accomplished for only one of a myriad of combinations of system parameters, initial conditions and boundary conditions. Proper validation will require additional physical experiments and numerical analysis to be performed in which key system parameters are systematically varied and measured, within the bounds encountered in the

natural system, to evaluate their effect on system response. As a step in this direction, we are in the process of comparing numerical simulation to our experimental data.

We must note that numerous other sub-processes governing fracture-matrix interaction that operate both in the plane and normal to the plane of the fracture[9,10,11,12,13,14] must be explored before large-scale effective media models that include fracture-matrix interaction may be adequately assessed.

CONCLUSION

Two preliminary experiments were conducted which provide insight into the processes governing fracture-matrix interaction in the plane normal to the fracture. Through these experiments we demonstrated the ability of the full-field x-ray absorption technique to acquire two-dimensional saturation and solute concentration fields in heterogeneous fractured media. Further improvement of the x-ray imaging technique is being pursued that will greatly enhance experimental capabilities. For instance, the use of medical angiography x-ray equipment is being explored. This equipment may be capable of bringing about a two- or three-fold increase in time resolution, as well as provide enhanced fracture imaging capabilities. The x-ray absorption technique also shows promise as a means of measuring porosity and sorptivity characteristics of heterogeneous media at high spatial resolution.

While Richard's equation was found to be a valid means of modeling matrix imbibition from a fracture for the discrete set of system parameters, boundary conditions and initial conditions used in the tuff experiment, such a simple test does not constitute model validation for all systems and boundary conditions. This work demonstrates both the need for and the capability to conduct systematic physical and numerical experimentation aimed at developing models for quantifying fracture-matrix interaction.

ACKNOWLEDGMENTS

The authors' extend their appreciation to Chris

Rautman for his help in measuring sample porosities, David Broxton for his petrographic description of our tuff sample, Kerim Martinez and Craig Ginn for their help in flow chamber fabrication, Lee Orear for help in coding various analysis tools, and Deanna Sevier for her help in acquiring the x-ray images. This work was supported by the U.S. Department of Energy, Office of Civilian Radioactive Waste Management, Yucca Mountain Site Characterization Project, under contract DE-AC4-76DP00789.

REFERENCES

1. R. R. PETERS and E. A. KLAVETTER, "A Continuum Model for Water Movement in an Unsaturated Fractured Rock Mass," Water Resources Research, 24, 416-430 (1988).

2. I. NERETNIEKS, and A. RASMUSON, "An approach to modeling radionuclide migration in a medium with strongly varying velocity and block sizes alone the flow path" Water Resources Research, 20, 1823-1836 (1984).

3. R. W. ZIMMERMAN, G. S. BODVARSSON, and E. M. KWICKLIS, " Absorption of Water into Porous Blocks of Various Shapes and Sizes," Water Resources Research,26,.2797-2806 (1990).

4. M. J. MARTINEZ, "Capillary Driven Flow in a Fracture Located in a Porous Medium," SAND84-1697, Sandia National Laboratory (1988).

5. T. A. BUSCHECK and J. J. NITAO, "Estimates of the Width of the Wetting Zone Along a Fracture Subjected to an Episodic Infiltration Event in Variably Saturated, Densely Welded Tuff," UCID-2157900, Lawrence Livermore National Laboratory (1988).

6. R. J. GLASS, "Laboratory Research Program to Aid in Developing and Testing the Validity of Conceptual Models for Flow and Transport Through Unsaturated Porous Media," Proceedings of the Geoval'90 Symposium, Stockholm, Sweden (1989).

7. R. J. GLASS and V. C. TIDWELL, "Research Program to Develop and Validate Conceptual Models for Flow and Transport Through Unsaturated, Fractured Rock," in Proceedings of the Second Annual International High Level Radioactive Waste Management Conference, Las Vegas, 2, 977-987

(1991).

8. A. J. RUSSO and D. C. REDA, "Drying of and Initially Saturated Fractured Volcanic Tuff," Journal of Fluids Engineering, 3, 191-196 (1989).

9. R. J. GLASS, and D. L. NORTON, "Wetted-Region Structure in Horizontal Unsaturated Fractures: Water Entry Through the Surrounding Porous Matrix," in the Proceedings of the Third Annual International High Level Radioactive Waste Management Conference, Las Vegas, 1, 717-726 (1992).

10. M. J. NICHOLL, R. J. GLASS, and H. A. NGUYEN, "Gravity-Driven Fingering in Unsaturated Fractures," in the Proceedings of the Third Annual International High Level Radioactive Waste Management Conference, Las Vegas, 1, 321-331 (1992).

11. M. J. NICHOLL, R. J. GLASS, and H. A. NGUYEN, "Wetting Front Instability in an Initially Dry Fracture," in the Proceedings of the Fourth Annual International High Level Radioactive Waste Management Conference, Las Vegas (1993).

12. M. J. NICHOLL, R. J. GLASS, and H. A. NGUYEN, "Small-Scale Behavior of Single Gravity-Driven Fingers in an Initially Dry Fracture," in the Proceedings of the Fourth Annual International High Level Radioactive Waste Management Conference, Las Vegas (1993).

13. D. P. GALLEGOS, S. G. THOMA, and D. M. SMITH, "Impact of Fracture Coatings on the Transfer of Water Across Fracture Faces in Unsaturated Media," in the Proceedings of the Third Annual International High Level Radioactive Waste Management Conference, Las Vegas, 1, 738-745 (1992).

14. T. C. RASMUSSEN, "Bypass Flow Through Unsaturated Fractured Rock: Effective Models for Fracture-Matrix Interactions," The AGU 1992 Fall Meeting Abstract Supplement, H32A-11 (1992).

15. V. C. TIDWELL and R. J. GLASS, "X-ray and Visible Light Transmission as Two- Dimensional, Full-Field Moisture-Sensing Techniques: A Preliminary Comparison," in the Proceedings of the Third Annual International High Level Radioactive Waste Management Conference, Las

Vegas, 1, 1099-1110 (1992).

16. R. J. GLASS, T. S. STEENHUIS, and J.-Y. PARLANGE, "Wetting Front Instability II: Experimental Determination of Relationships Between System Parameters and Two Dimensional Unstable Flow Field Behavior in Initially Dry Porous Media," Water Resources Research, 25, 1195-1207 (1989.

Figures:

1). Flow chamber. Above, exploded view of flow chamber assembly showing porous plates, plastic laminant, parafilm, and aluminum frame. Below, flow chamber and calibration step-wedge placed transversely in x-ray beam between x-ray generator and film cassette.

2). Analog system saturation fields at a) 234, b) 397, c) 565, and d) 730 seconds. In these images, white signifies 100% saturation grading to black corresponding to initial saturation (oven dry). Vertical flow in the matrix is evidenced by the uneven vertical propagation of the flow field on either side of the fracture.

3). Tuff system saturation fields at a) 123, b) 957, c) 1890, and d) 3903 seconds. In these images, white signifies 100% saturation grading to black corresponding to initial saturation (oven dry). Note that in the first image imbibition is evident along the full length of the fracture indicating that the fracture transmitted water from very early times in the experiment.

4). Comparison of the total volume of water in the analog system as measured by gravimetric methods and estimated from x-ray images.

5). Analog solute concentration fields at a) 150, b) 317, c) 491, and d) 821 seconds. In these four images the grey scale qualitatively references solute concentration, with white signifying a concentration of 10% KI, while black corresponds to pure DeI.

6) Tuff system saturation transects for times between 123 and 3903 seconds.

7) Lateral distance from the fracture (d) where the tuff matrix has reached 50% saturation as a function of the square root of time.

8) Infiltration volume per cross-section of fracture (I) imbibed by tuff as a function of the square root of time.

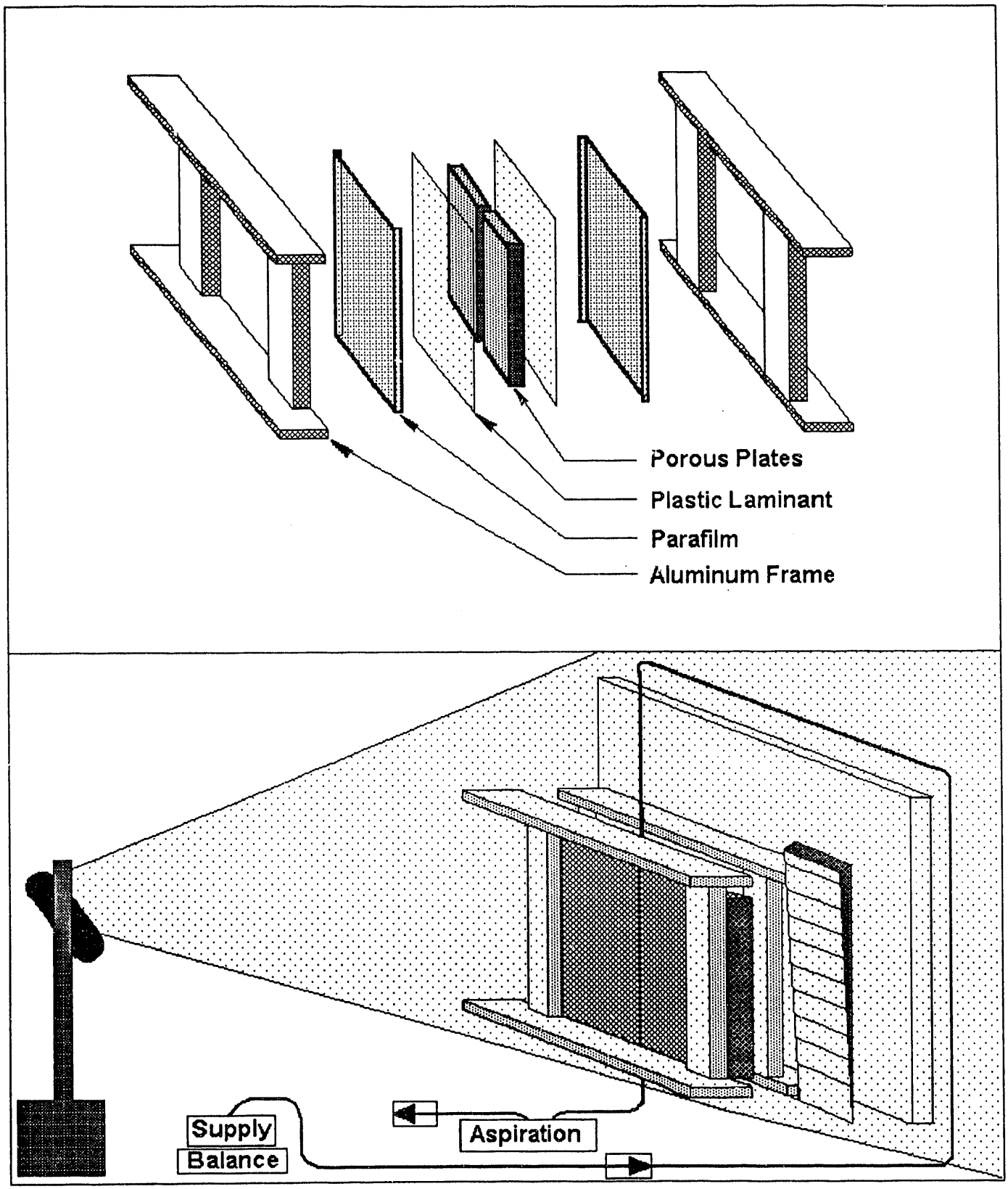
Porous Plates
Plastic Laminant
Parafilm
Aluminum Frame
Supply
Balance
Aspiration

Figure 1

$\tau_{run} = 234s$

Figure 2a

$t_{run} = 347\,s$

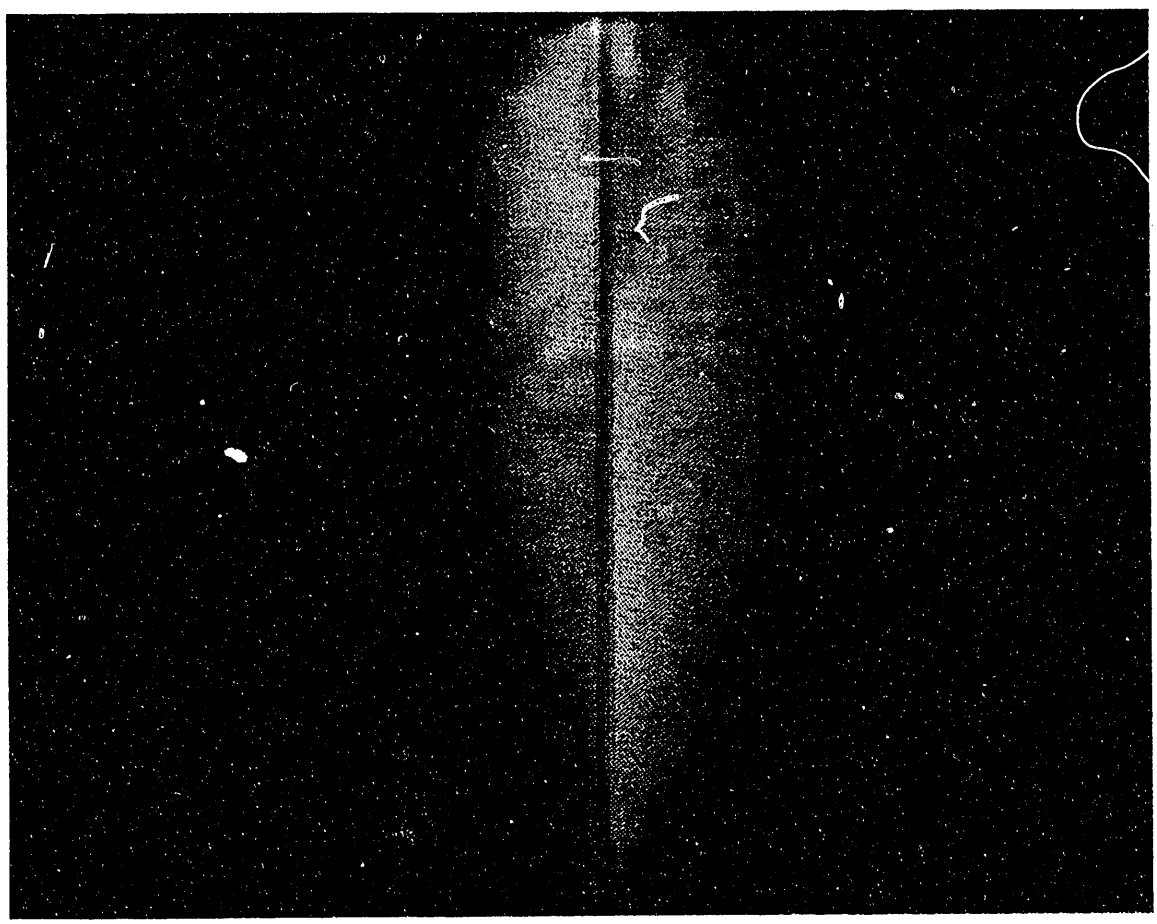

Figure 2.b

$t_{run} = 565\ s$

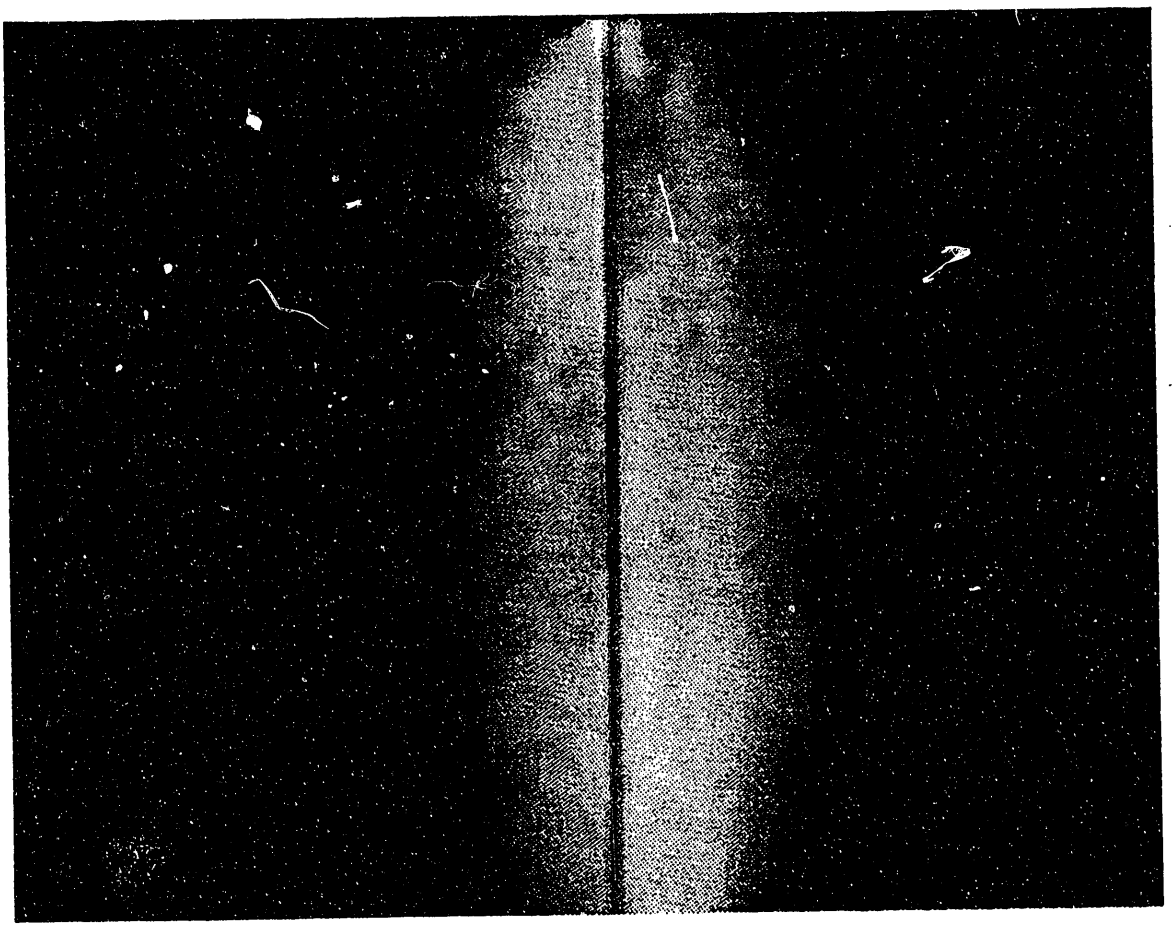

Figure 2C

t_{run}
$= 730\ s$

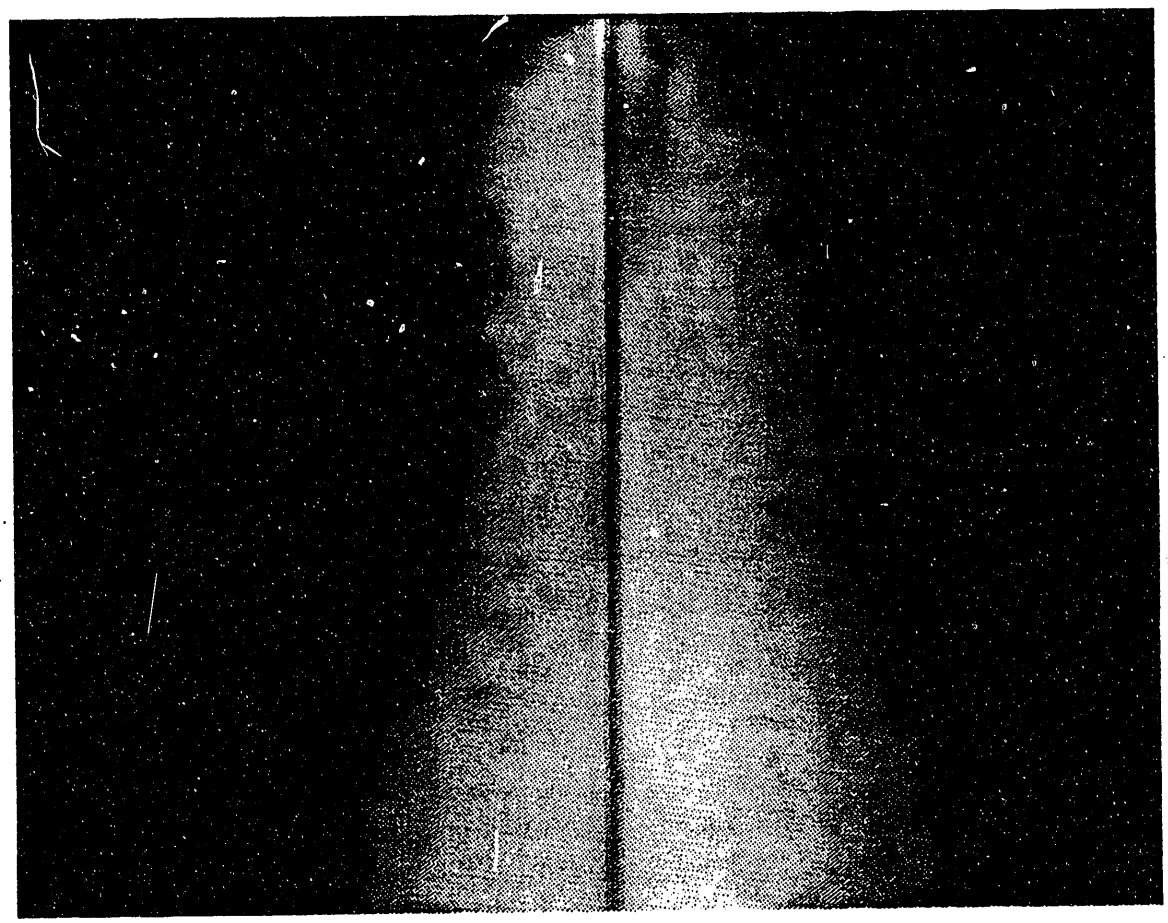

Figure 2d

run = 1235

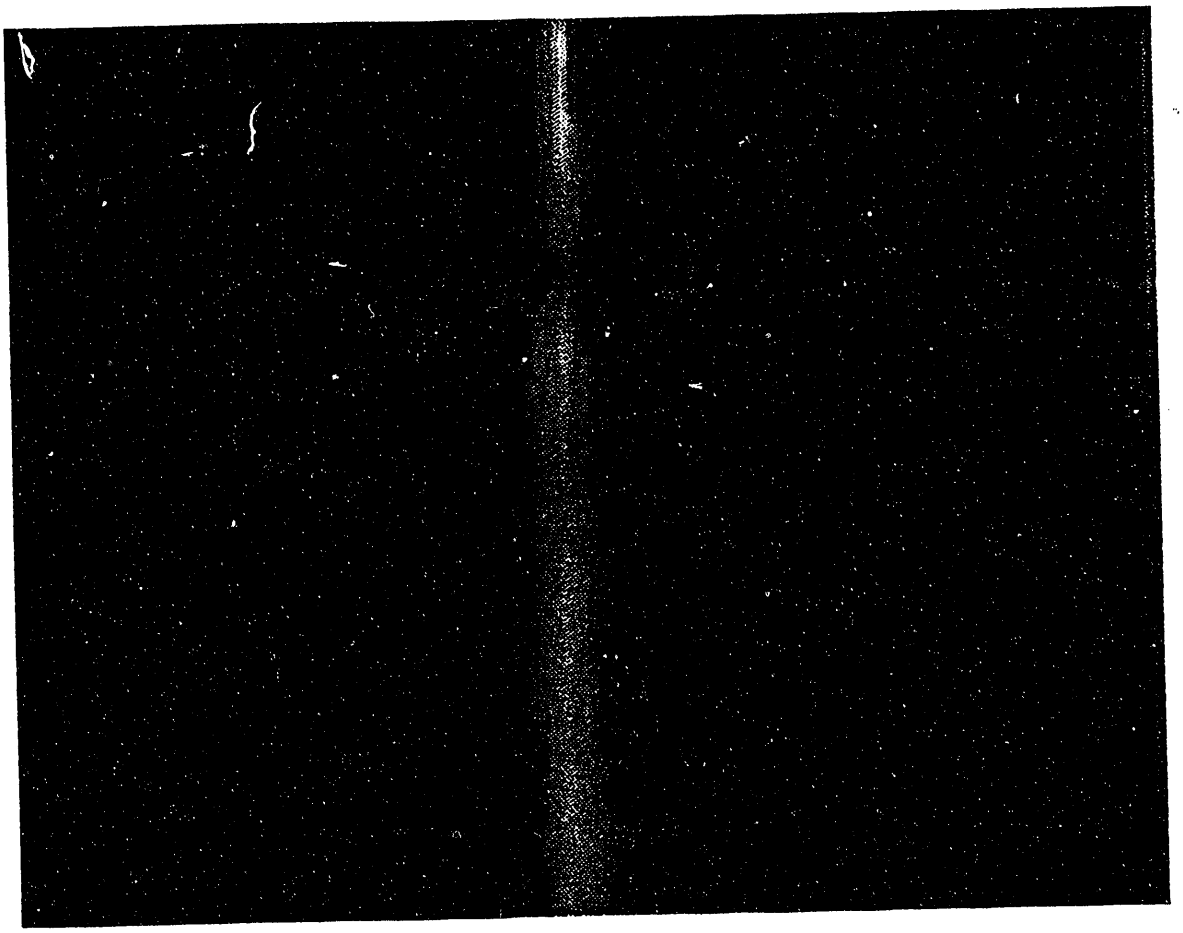

Figure 3a

Lrun
= 957s

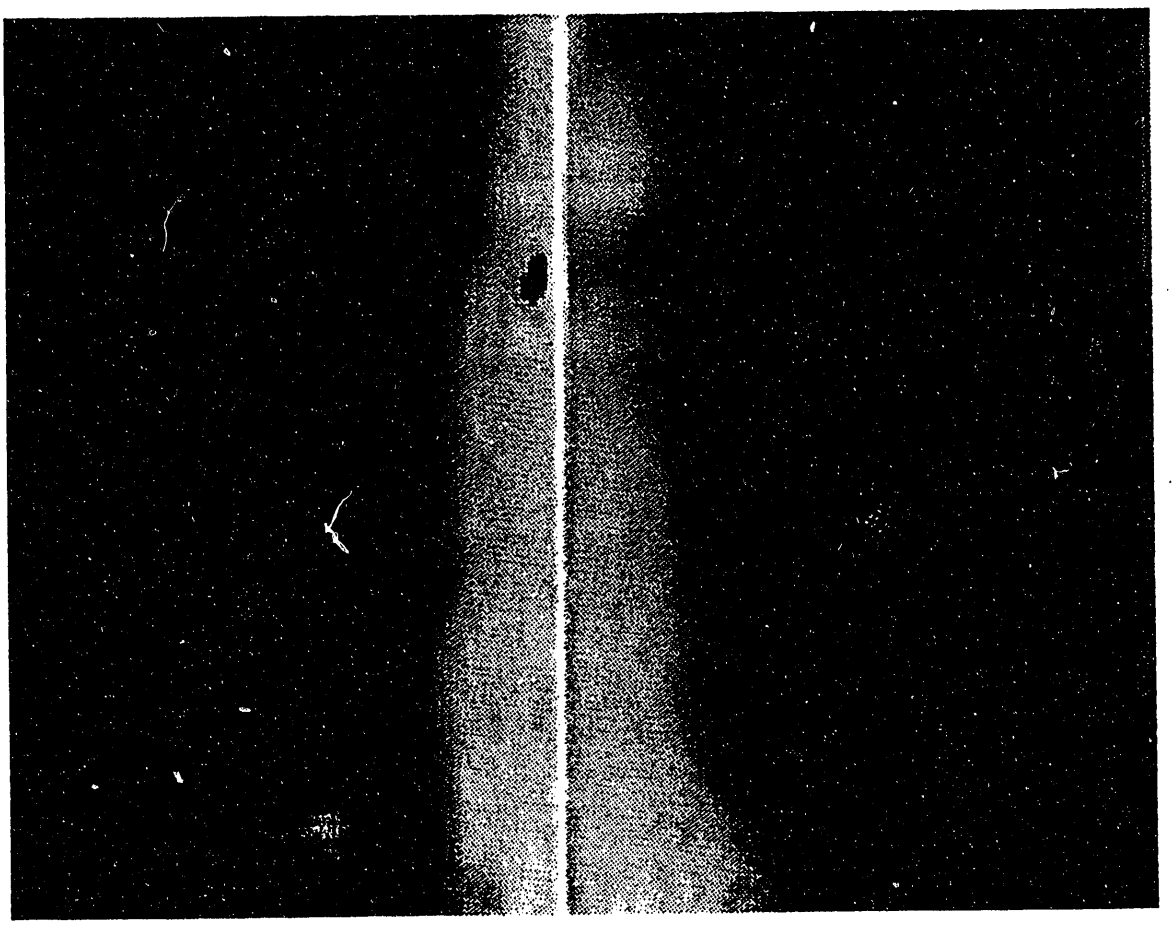

Figure 3 b

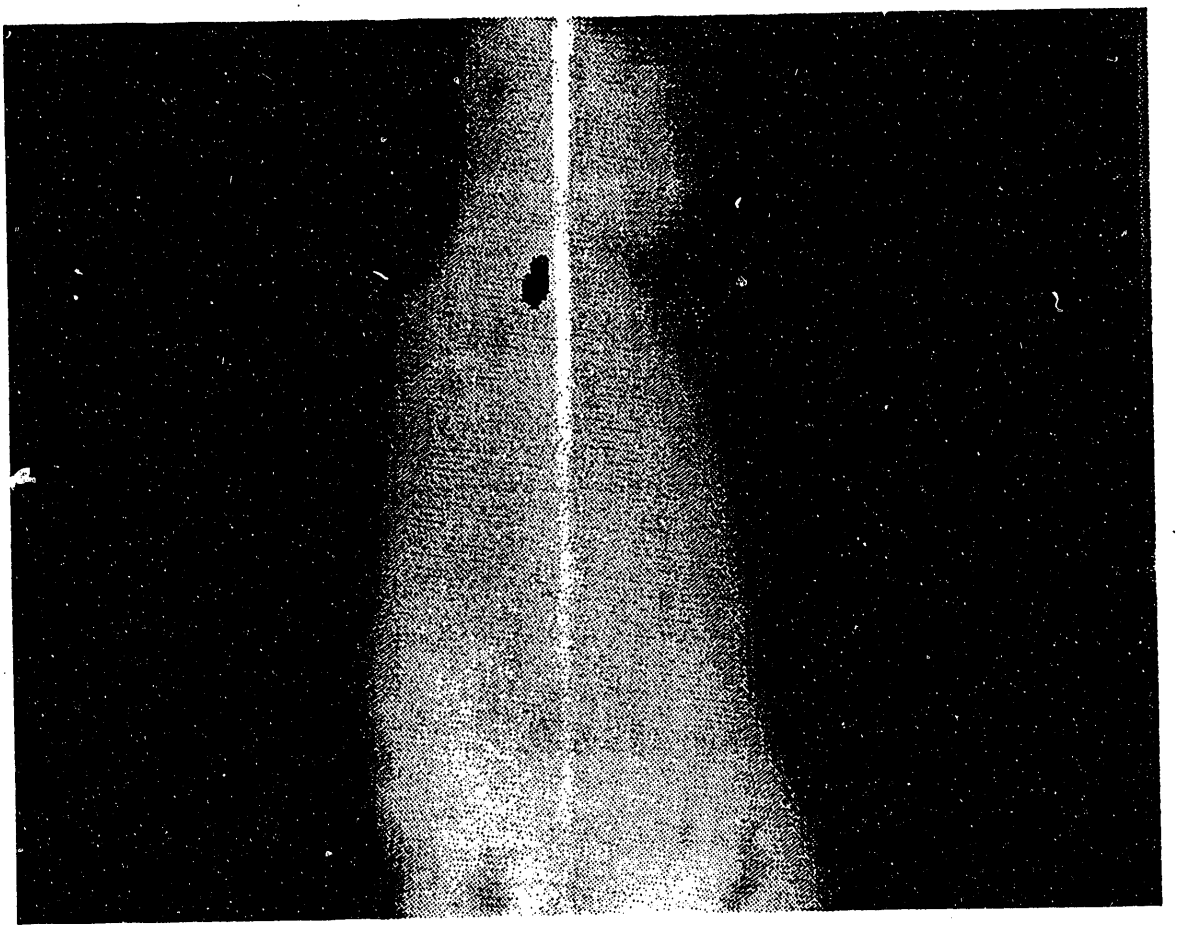

Figure 3C

Run = 3703 S

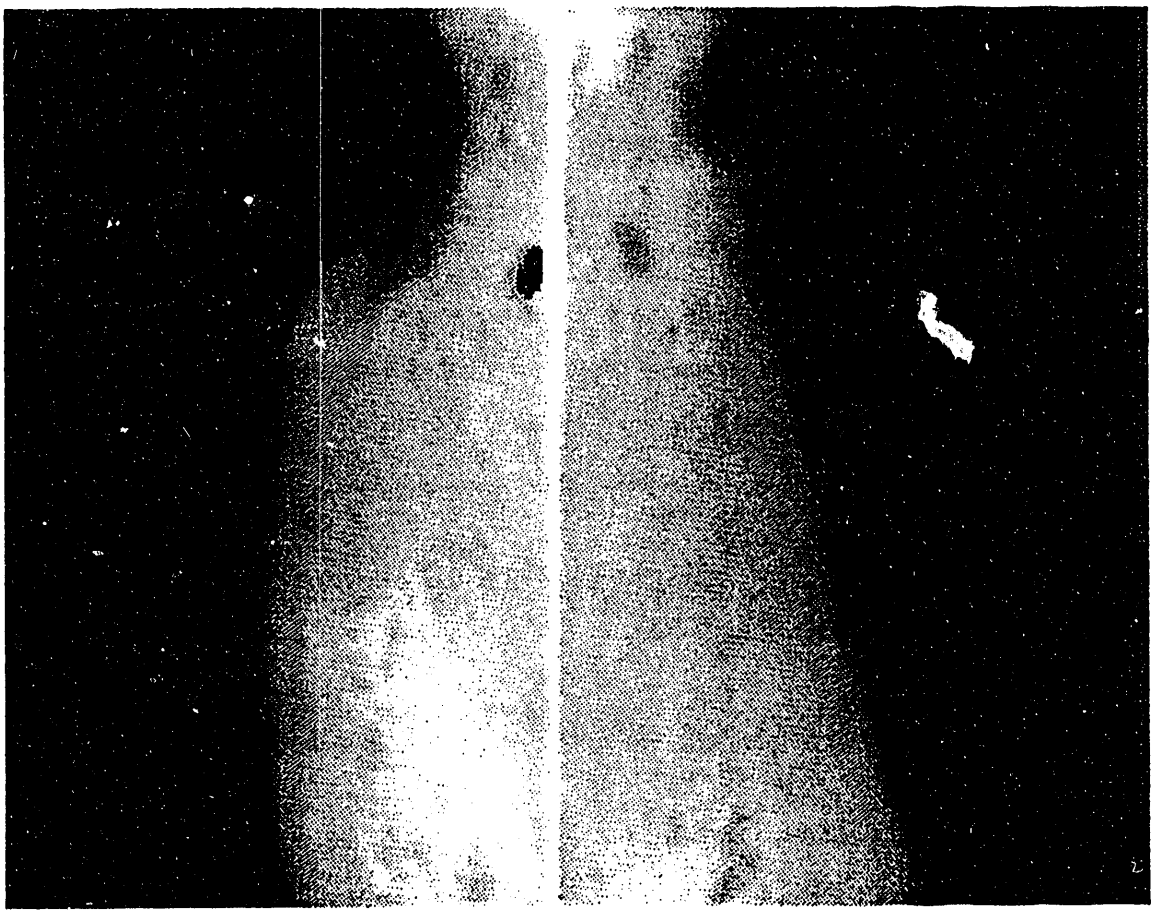

Figure 3 d

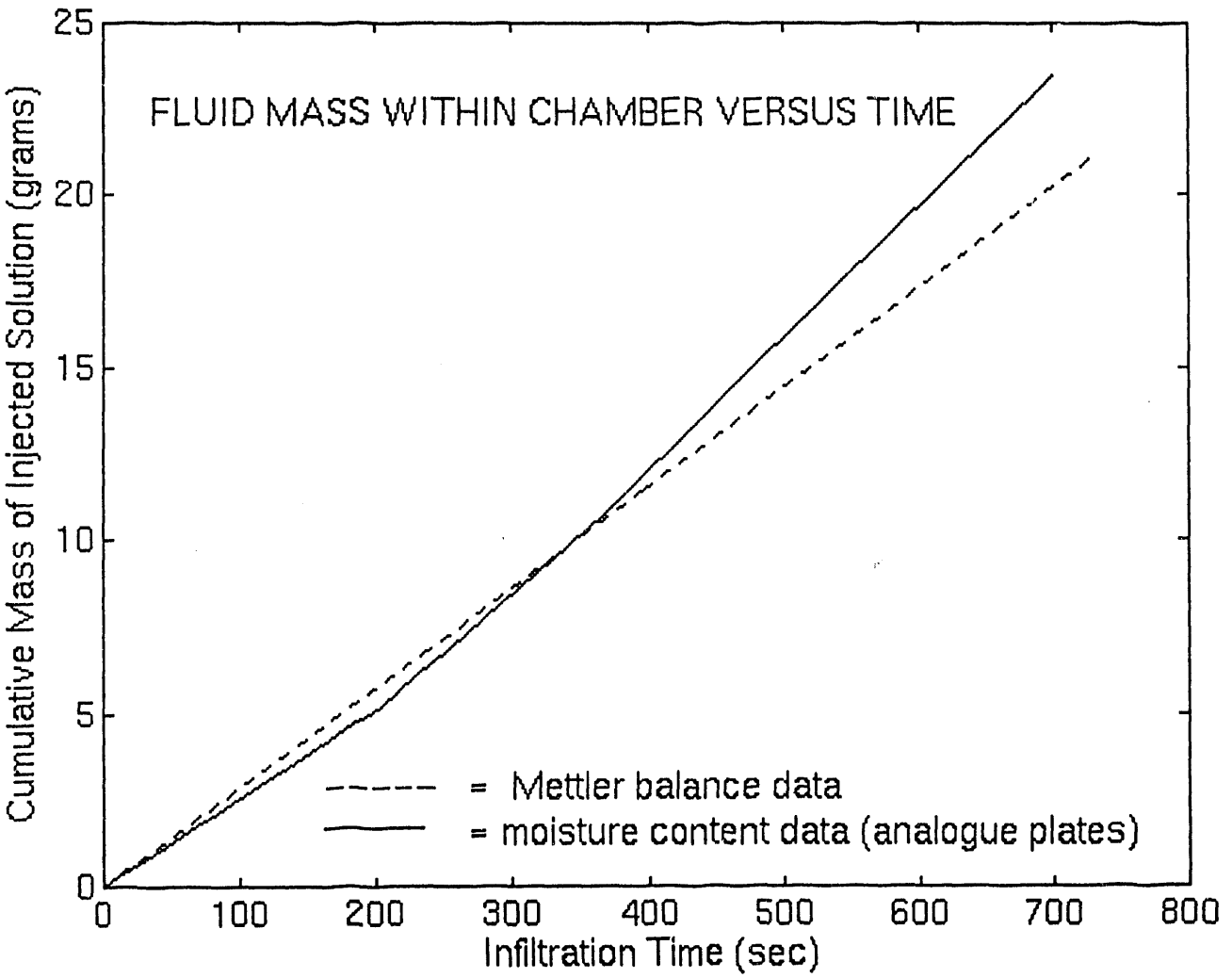
FLUID MASS WITHIN CHAMBER VERSUS TIME
Cumulative Mass of Injected Solution (grams)
Infiltration Time (sec)
= Mettler balance data
= moisture content data (analogue plates)
0
5
10
15
20
25
0
100
200
300
400
500
600
700
800

Figure 4

$t_{flush} = 150s$

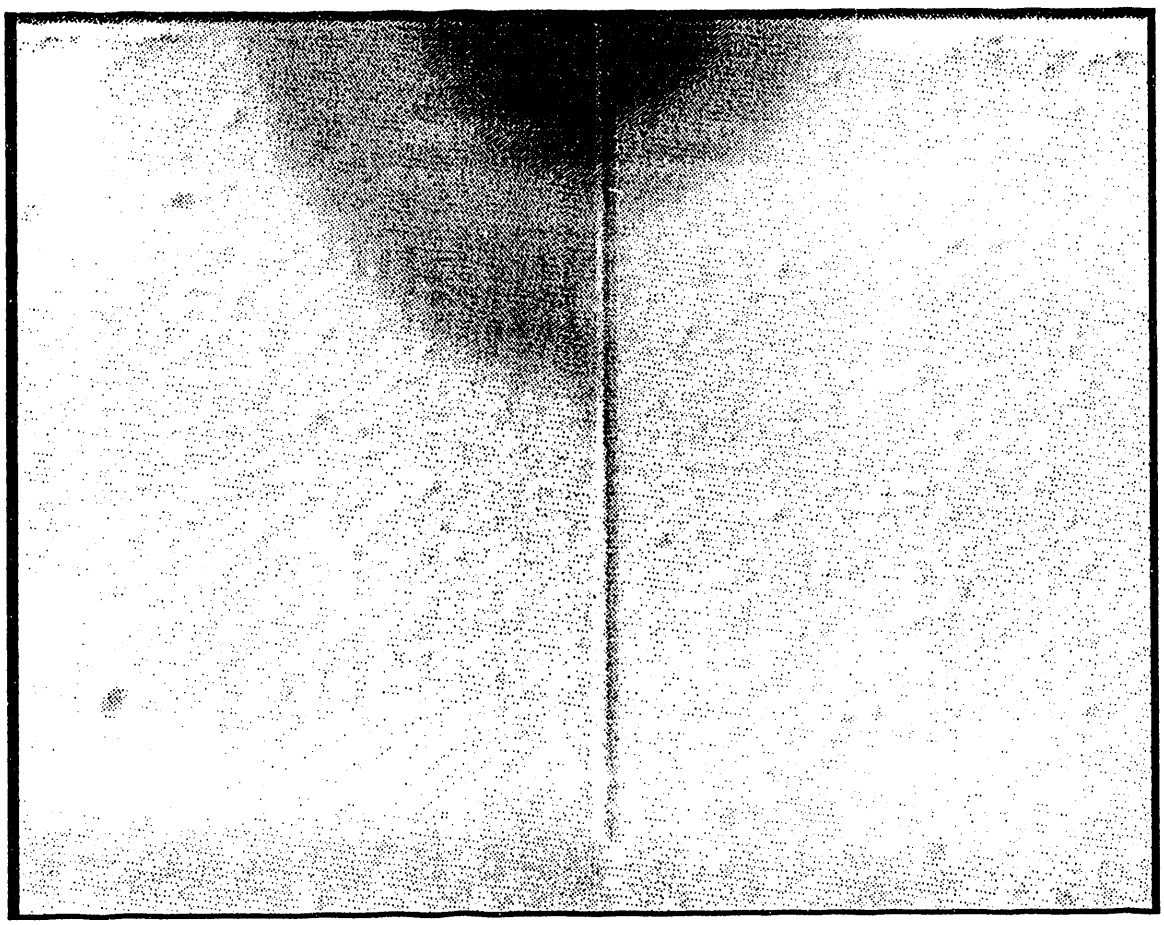

Figure 5a

$t_{flash} = 317\ s$

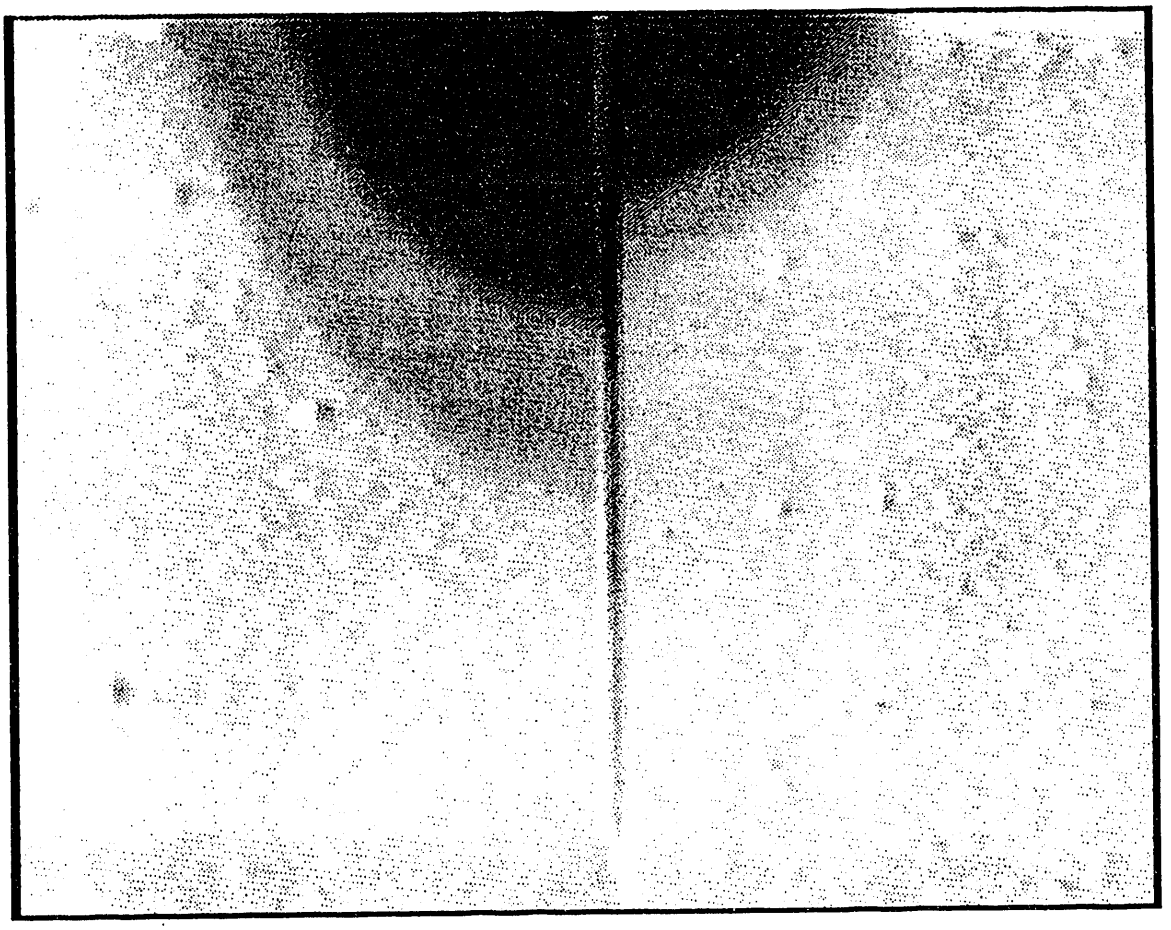

Figure 5*b

$t_{flush} = 491 s$

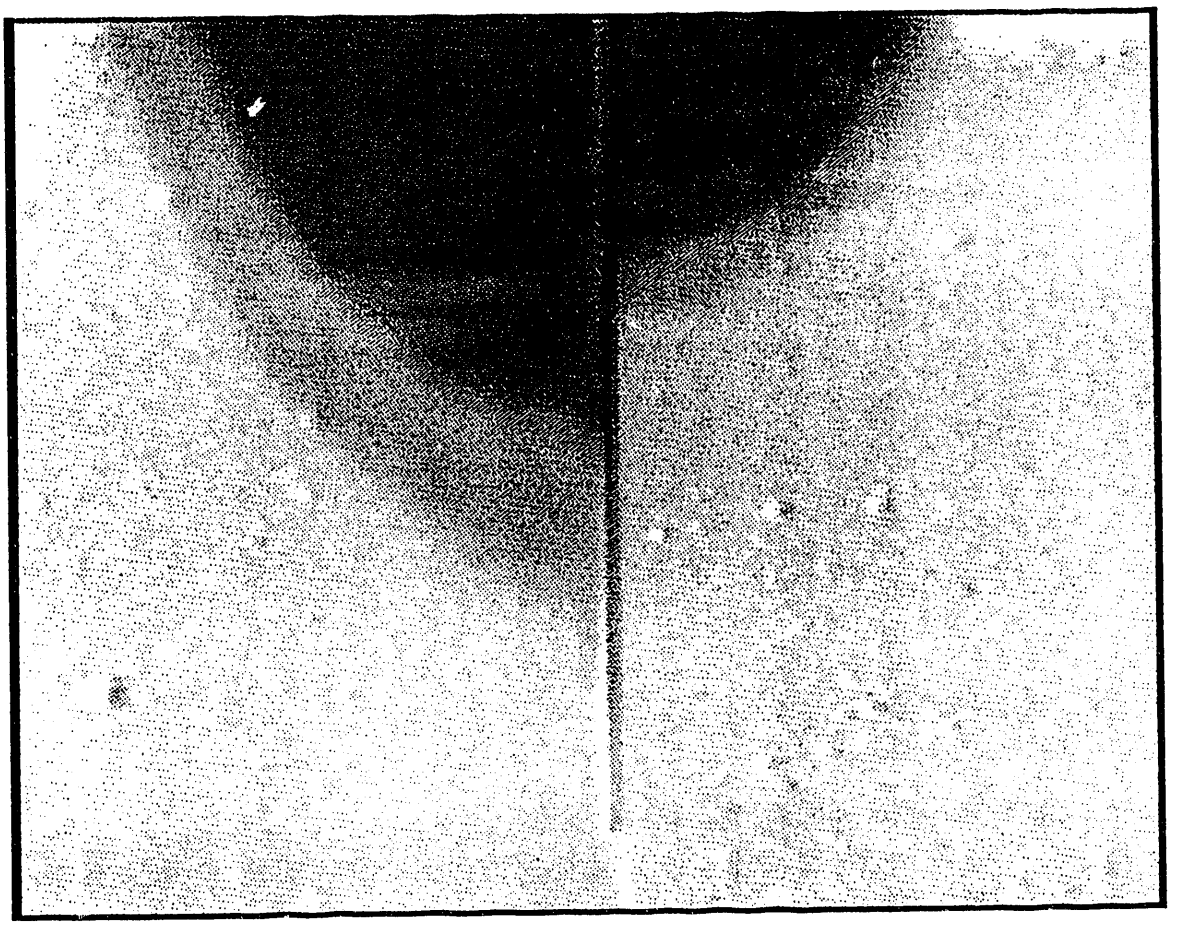

Figure 5c

$t_{flush} = 82 s$

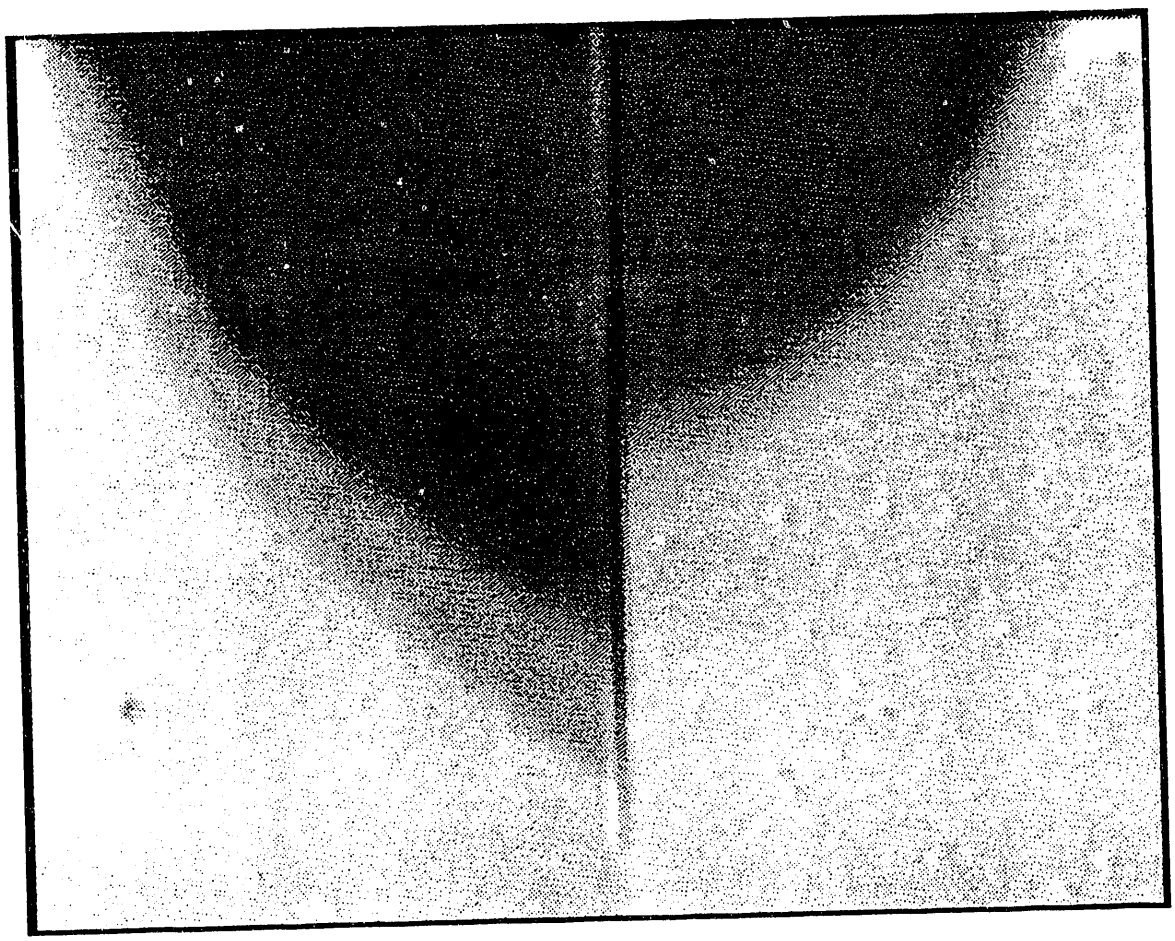

Figure 5d

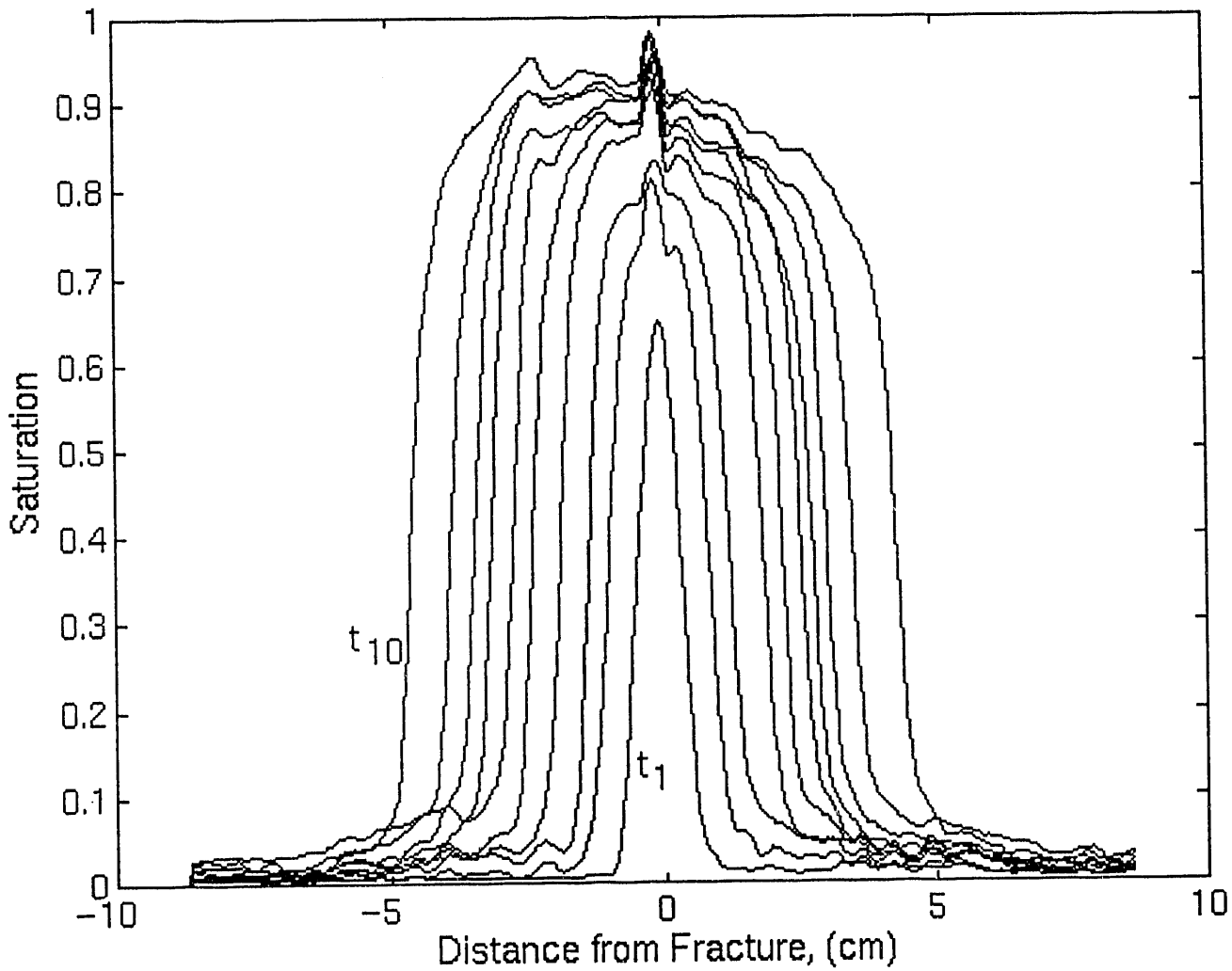
Saturation
Distance from Fracture, (cm)
t10
t1
1
0.9
0.8
0.7
0.6
0.5
0.4
0.3
0.2
0.1
0
−10
−5
0
5
10

Figure 6

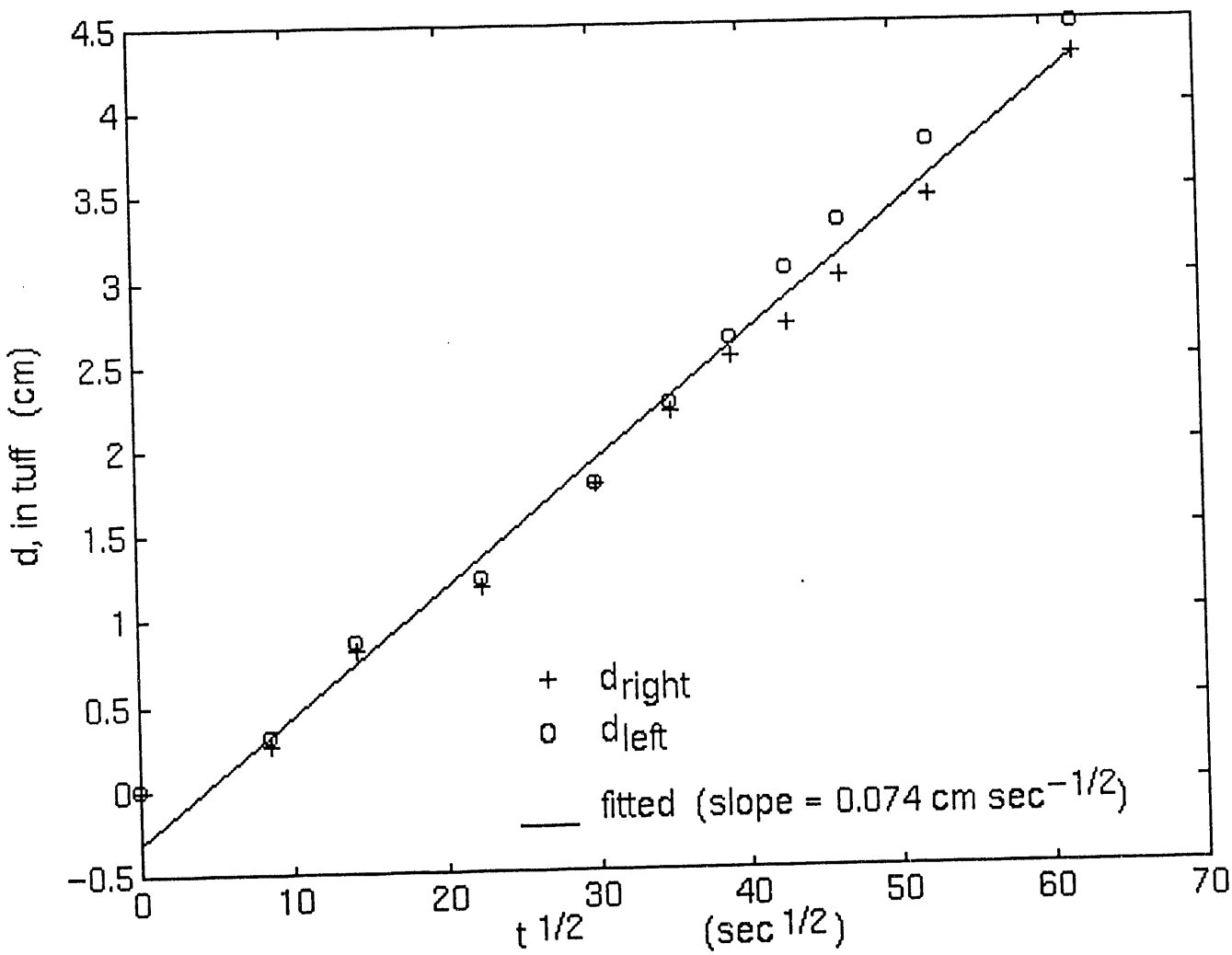
4.5
4
3.5
3
2.5
2
1.5
1
0.5
0
−0.5
0
10
20
30
40
50
60
70
d, in tuff (cm)
t 1/2 (sec 1/2)
+ d right
o d left
fitted (slope = 0.074 cm sec−1/2)

Figure 7

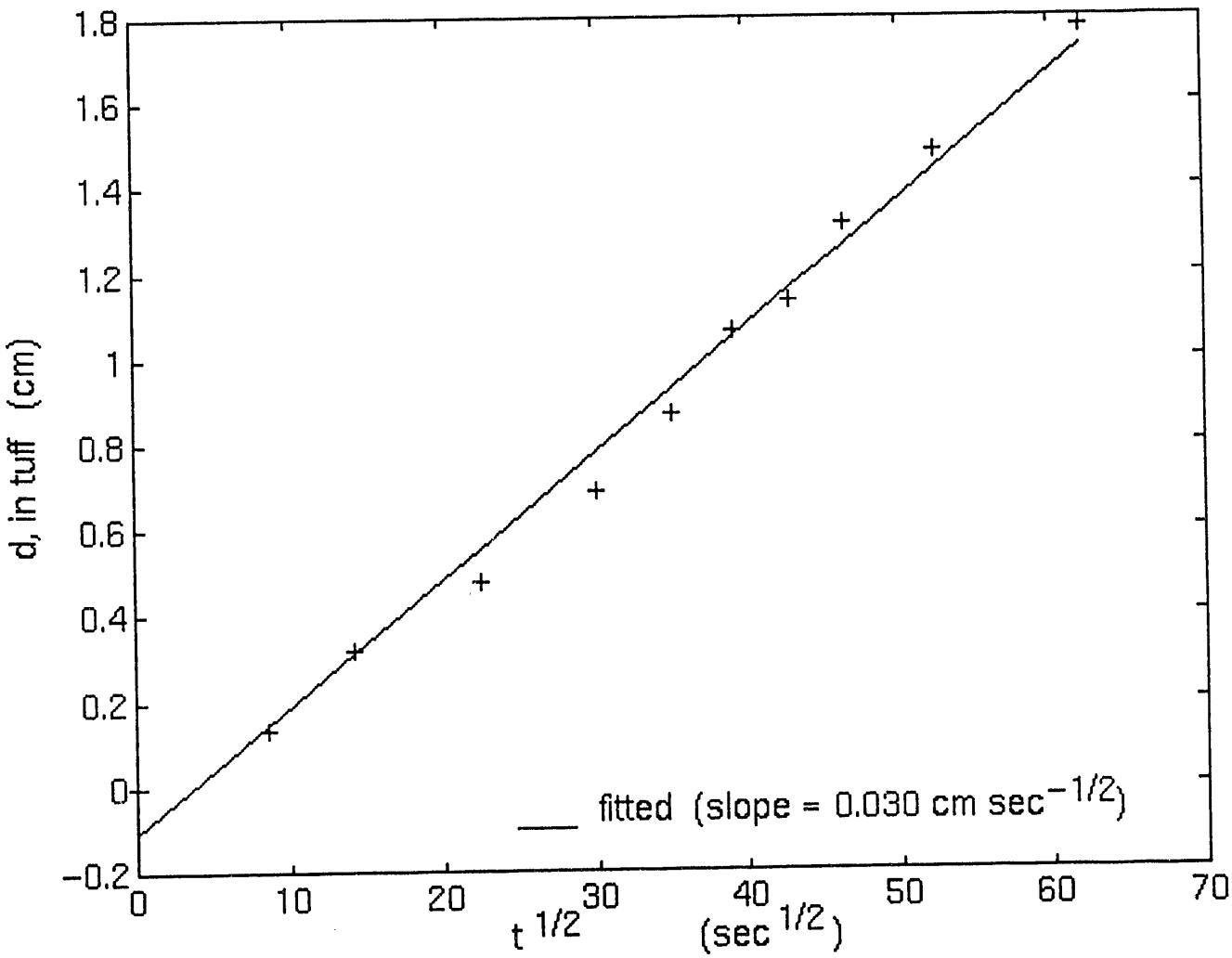
1.8
1.6
1.4
1.2
1
0.8
0.6
0.4
0.2
0
−0.2
d, in tuff (cm)
0
10
20
30
40
50
60
70
t 1/2
(sec 1/2)
fitted (slope = 0.030 cm sec−1/2)

Figure 8

END

DATE
FILMED
6/23/93